EDDY CURRENTS

INTRODUCTION

Changing magnetic fields produce an electric field. This fact was discovered about 150 years ago independently by Michael Faraday (1791–1868) (1) as well as Joseph Henry (1797–1878). That an electric current produces a magnetic field was discovered by Hans Christian Oersted (1777–1851) ten years earlier. Jean Bernard Léon Foucault (1819–1868), a French physicist of considerable accomplishments, studied the nature of eddy currents by spinning a copper disk in a high magnetic field. Eddy currents are therefore also referred to as Foucault's currents. It is the interactions of magnetic fields and electric currents that have given rise to a myriad of applications that make modern civilization possible.

In the phenomenon of eddy currents, the varying magnetic field is present as well as the induced current and its magnetic field. For example, when a loop of wire experiences a magnetic field which varies with time, then a voltage is induced in that wire (this is termed Faraday's law). If this wire encloses the changing magnetic field so that a complete circuit is present, then a current flows in the wire. The current in the wire in turn produces its own magnetic field. This interaction is exploited in devices such as generators and transformers. If the conducting medium is not a filamentary wire but a conductor of substantial size, then the effect of the time varying magnetic fields on the conductor is more complex. The induced currents now do not have a prescribed path and therefore will flow in patterns consistent with the applied magnetic field distribution. These patterns of induced currents are termed eddy currents.

The eddy currents in most conventional devices are accompanied by a loss in energy. If the eddy currents are permitted to flow unabated, they reduce the strength of the applied magnetic field as well as produce undesirable forces. The cores of transformers and generators are laminated (made of thin sheets of ferromagnetic material) rather than monolithic pieces to break up the eddy current path and reduce the negative effects. The same effects cause nonuniform distribution of current in conductors at high frequencies, thus resulting in higher energy losses than that obtained by considerations of the dc resistance of the conductor.

J. Webster (ed.), *Wiley Encyclopedia of Electrical and Electronics Engineering*. Copyright © 1999 John Wiley & Sons, Inc.

Applications of Eddy Currents

There are several devices that exploit the presence of eddy currents and put them to good use. An example is the induction motor/generator. The induction machine is a robust device finding use in homes as well as industry. The rotor of the induction machine is in the form of a cup or a squirrel cage made from a good conductor. This construction does not need brushes and slip rings on the rotor to collect current from an external source, which contributes to its ruggedness. The current in the rotor is entirely induced by interactions with the changing stator magnetic field. The interactions between rotor and stator produce a torque that can be tailored to an application.

When a sufficiently high-frequency current flows through a conductor there is a tendency for the current to flow in a small cross section on the surface of the conductor, i.e., the "skin" of the conductor. This is termed the *skin effect* (2). This fact is exploited in induction heating of parts so that the heat treatment is applied only to the surface. The depth to which the heating is accomplished can be controlled by the frequency of the applied magnetic field. The skin effect is observed because the high-frequency current (which the conductor is carrying) produces a changing magnetic field that in turn induces eddy currents in the conductor in such a manner that the changing magnetic field is excluded from the conductor.

Electrodynamic levitation is being considered for trains (3). In this mechanism the train carries on board a series of magnets. As the train moves, these magnets induce eddy currents on the track conductors. The interaction of the current in the tracks and the resultant magnetic field produces a levitation force.

The exploration of space has relied on chemical energy in rockets for propulsion. This method of propulsion has reached its ultimate potential, and new, cheaper methods need to be devised. An alternative is electromagnetic launching. A variant of electromagnetic launchers uses eddy currents induced in a shuttle by a series of stationary coils. This launcher can best be described as a linear induction machine.

There are several other useful applications that eddy currents can be put to, such as nondestructive evaluation of conducting parts, since the eddy currents carry information about the material in which they flow.

GOVERNING EQUATIONS

James Clerk Maxwell (1831–1879) summarized the behavior of the electromagnetic field in a set of equations now named after him (4). These are summarized below:

$$\nabla \times \boldsymbol{H} = \boldsymbol{J}_f + \frac{\partial \boldsymbol{D}}{\partial t} \qquad \text{(Ampere's law)} \tag{1}$$

$$\nabla \times \boldsymbol{E} = -\frac{\partial \boldsymbol{B}}{\partial t} \qquad \text{(Faraday's law)} \tag{2}$$

$$\nabla \cdot \boldsymbol{D} = \rho_f \qquad \text{(Gauss's law)} \tag{3}$$

$$\nabla \cdot \boldsymbol{B} = 0 \tag{4}$$

Here the symbols have the usual meanings: $\boldsymbol{H}$ (A/m) is the magnetic field intensity; $\boldsymbol{B}$ (T) is the magnetic flux density; $\boldsymbol{E}$ (V/m) is the electric field strength; and $\boldsymbol{D}$ (C/m^2) the electric flux density. $\boldsymbol{J}_f$ is the free current density in A/m^2 and ρ_f is the free charge density in coulombs/m^3. All these quantities will be used in their MKS units throughout this article. These equations are presented here in their most general form. They describe the phenomenon of wave propagation. The phenomenon of eddy currents is usually restricted to low frequencies. This regime of the electromagnetic field is referred to as the quasistatic regime. In the quasistatic (5) regime there is no wave propagation and the term $\partial \boldsymbol{D}/\partial t$ in Eq. (1), also referred to as the displacement current, can be neglected. If ω is the applied frequency in radians per second, l is the maximum dimension of the device under consideration, and c is velocity of light, then the condition $\omega l/c \ll 1$ must be satisfied if the quasistatic set of equations is to be used.

In the quasistatic regime the four applicable equations are as follows:

$$\nabla \times \boldsymbol{H} = \boldsymbol{J}_f \tag{5}$$

$$\nabla \times \boldsymbol{E} = -\frac{\partial \boldsymbol{B}}{\partial t} \tag{6}$$

$$\nabla \cdot \boldsymbol{B} = 0 \tag{7}$$

$$\nabla \cdot \boldsymbol{J}_f = 0 \tag{8}$$

It must be noted that the last two equations are not entirely independent of the first two, as they can be obtained by taking the divergence of Eqs. (5) and (6). These equations, along with material properties such as conductivity σ (S/m) and permeability μ_0 [Wb/(A/m)] and the constitutive relations, can be combined to give the diffusion equation. The constitutive relations for linear isotropic materials are as follows:

$$\boldsymbol{B} = \mu_0 \boldsymbol{H} \tag{9}$$

$$\boldsymbol{J}_f = \sigma \boldsymbol{E} \qquad \text{(Ohm's law)} \tag{10}$$

Taking the curl of Eq. (5), we get

$$\nabla \times \nabla \times \boldsymbol{H} = \nabla(\nabla \cdot \boldsymbol{H}) - \nabla^2 \boldsymbol{H} = \nabla \times \boldsymbol{J}_f \tag{11}$$

Using the constitutive relations and Eqs. (6) and (7) in (11), we get the magnetic diffusion equation:

$$\nabla^2 \boldsymbol{H} = \mu_0 \sigma \frac{\partial \boldsymbol{H}}{\partial t} \tag{12}$$

Thus it is shown that the magnetic field obeys the vector diffusion equation with the eddy current phenomenon.

Diffusion is a process commonly observed in nature. It is the process by which matter is transported from one part of a system to another as a result of random molecular motions. Diffusion is also observed in the transfer of heat by conduction between a hot and a cold object. Initially when the hot and cold objects are brought together, there exists a clear boundary at the interface. As time progresses the flow of heat brings the two bodies closer in temperature. Similarly, Eq. (12) indicates that if a magnetic field is established around a conductor it will not be felt instantaneously in the interior of the conductor, but will slowly establish itself as the eddy currents on the surface of the conductor decay. Since Eq. (12) is a vector equation, it must be solved for the three components. Solving Eq. (12) for $\boldsymbol{H}$, the magnetic field intensity, requires

the use of the boundary and initial conditions that are appropriate for the problem. Equation (5) is then used to calculate the current density distribution. The current density also obeys the vector diffusion equation.

Equation (12) assumes that the conducting material is at rest with respect to the coordinate reference frame. When the conducting body is in motion with respect to the coordinate frame, then Eq. (12) is modified to what is termed the convective diffusion equation. In the conductor moving with a velocity $\boldsymbol{v}$ (m/s) with respect to the coordinate reference frame, Faraday's law is modified to (6)

$$\nabla \times \boldsymbol{E} = -\frac{\partial \boldsymbol{B}}{\partial t} + \nabla \times (\boldsymbol{v} \times \boldsymbol{B}) \tag{13}$$

Starting with Eq. (11), using Ohm's law and substituting Eq. (13) for $\nabla \times \boldsymbol{E}$, the following equation is obtained:

$$\nabla^2 \boldsymbol{H} = \mu_0 \sigma \left[\frac{\partial \boldsymbol{H}}{\partial t} - \nabla \times (\boldsymbol{v} \times \boldsymbol{H}) \right] \tag{14}$$

If the velocity is the same at all points of the conductor, then Eq. (14) becomes

$$\nabla^2 \boldsymbol{H} = \mu_0 \sigma \left[\frac{\partial}{\partial t} + \boldsymbol{v} \cdot \nabla \right] \boldsymbol{H} \tag{15}$$

The right-hand side of Eq. (15) is the rate of change with respect to time for an observer moving with a velocity $\boldsymbol{v}$ of the conductor. This convective derivative represents two ways in which a conductor may experience a time rate of change of magnetic field. One is due to a time-varying source field, and the second is due to the motion of the conductor through a spatially varying field. Two constants emerge from Eq. (15): one is the magnetic diffusion time $\tau_m = \mu_0 \sigma d^2$; and the other is the magnetic Reynolds number $R_m = \mu_0 \sigma v d$. Here d is a typical length of the device.

SKIN EFFECT

To illustrate the concept of the skin effect, a simple one-dimensional example is given. This also allows one to apply some of the equations derived in the previous section. A semi-infinite conductor occupying the entire positive x plane is shown in Fig. 1. It is assumed to have the permeability of free space and conductivity σ. The assumptions of infinite dimensions in the y, z, and positive x directions allows the problem to be solved in one dimension. The excitation is in the form of a time-harmonic magnetic field $H = H_0 \cos(\omega t)$, at $x = 0$, directed along the positive y direction. The field quantities will be a function of only time and the x coordinate. Equation (12) now reduces to the simple one-dimensional diffusion equation

$$\frac{\partial^2 H_y}{\partial x^2} = \mu_0 \sigma \frac{\partial H_y}{\partial t} \tag{16}$$

Since the problem is time harmonic, it is assumed that the solution takes the form shown in Eq. (17). Here the tilde on H_y indicates the fact that it is now a complex number and $j = \sqrt{-1}$. The excitation frequency is denoted by ω:

$$H_y = \tilde{H}_y(x) e^{j\omega t} \tag{17}$$

The partial differential equation then reduces to the differential equation (18):

$$\frac{d^2 \tilde{H}_y}{dx^2} - j\omega \mu_0 \sigma \tilde{H}_y = 0 \tag{18}$$

The solution to (18) takes the form

$$\tilde{H}_y(x) = \tilde{C}_1 e^{\alpha x} + \tilde{C}_2 e^{-\alpha x} \tag{19}$$

Here

$$\alpha = \frac{1+j}{\delta}$$

and

$$\delta = \sqrt{\frac{2}{\omega \mu_0 \sigma}}$$

also called the *skin depth* or the *depth of penetration.*

Considering that the conductor stretches to infinity along the positive x direction, $\tilde{C}_1$ equals zero to keep the magnetic field finite in that region. Since at $x = 0, H_y = H_0 \cos(\omega t)$, then $\tilde{C}_2$ must equal H_0 and the complete solution takes the form

$$H_y(x,t) = H_0 e^{-x/\delta} \cos\left(\omega t - \frac{x}{\delta}\right) \tag{20}$$

This shows the relevance of the skin depth δ. It is the distance over which the magnitude of the field strength decays to 36.7% of its value at the surface. Equation (20) shows that the field amplitude not only decays but also retards in phase with depth into the conductor.

Equation (5) can now be used to determine the current density in the conductor. Performing the curl operation of Eq. (5) and realizing that the magnetic field has only one component, which is a function of only the x coordinate, the current density also has only one component, i.e., the z component:

$$J_z = \frac{\partial H_y}{\partial x} \tag{21}$$

From Eqs. (20) and (21) the current density is obtained as

$$J_z(x,t) = -\sqrt{\omega \mu_0 \sigma} H_0 e^{-x/\delta} \cos\left(\omega t - \frac{x}{\delta} + \frac{\pi}{4}\right) \tag{22}$$

The current density exhibits a behavior similar to the magnetic field, i.e., attenuating into the conductor and retarding

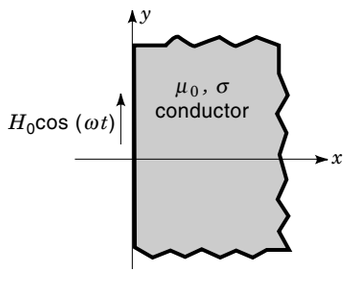

Figure 1. A semi-infinite conductor in the positive x-plane subject to a time harmonic field at $x = 0$.

Table 1. Depth of Penetration (Skin Depth) in Various Conductors

Conductor	Conductivity (S/m)	Relative Permeability	Skin Depth			
			At 60 Hz (cm)	At 1 kHz (mm)	At 1 MHz (mm)	At 3 GHz (μm)
Silver	6.15×10^7	1.00	0.83	2.03	0.064	1.17
Copper	5.80×10^7	1.00	0.85	2.09	0.066	1.21
Gold	4.50×10^7	1.00	0.97	2.37	0.075	1.37
Chromium	3.80×10^7	1.00	1.05	2.58	0.082	1.49
Aluminum	3.54×10^7	1.00	1.09	2.67	0.085	1.54
Zinc	1.86×10^7	1.00	1.51	3.69	0.117	2.13
Brass	1.59×10^7	1.00	1.63	3.99	0.126	2.30
Nickel	1.30×10^7	100	0.18	0.44	0.014	0.25
Magnetic iron	1.00×10^7	200	0.15	0.36	0.011	0.21
Tin	8.70×10^7	1.00	2.20	5.40	0.171	3.12
Mumetal	1.60×10^7	20,000	0.04	0.09	0.003	0.05
Graphite	1.00×10^7	1.00	20.55	50.33	1.592	29.06
Sea water	5.000	1.00	2905.76	7117.63	225.079	—

in phase. This is not surprising considering that the current density satisfies a partial differential equation identical to the magnetic field intensity, Eq. (16).

It must be noted that in this table the frequencies selected are fairly high (3 GHz). At the same time, since the very beginning displacement currents have been neglected. This is justified because in good conductors the conduction current density is still greater than the displacement current density. The ratio of the displacement current to the conduction current can be estimated by the ratio $\omega\epsilon/\sigma$ (7). Here ϵ is the electrical permittivity of the conductor. In free space the permittivity has a value of 8.854×10^{-12}. The ratio $\omega\epsilon/\sigma$ at 3 GHz for graphite, which is in the low range of conductivity (Table 1), is approximately 1.5×10^{-6}; thus the assumption of negligible displacement current density is validated. However, for water, which has a relative permittivity of 80 (8), this assumption is not valid at 3 GHz. The table therefore does not list the skin depth in water at that frequency.

So far the physics and the mathematics of eddy currents have been discussed. Now the physical conditions within the conductor that cause the current to flow on the skin of the conductor and repel the flux from the interior are discussed. The explanation is tied to Lenz's law, which is invariably related to Faraday's law [Eq. (2)].

Lenz's law simply states that whenever changes occur in a magnetic field, currents flow and forces act in a sense to oppose that change. To illustrate this, consider an infinitely long cylindrical conductor carrying a current along its axis, as shown in Fig. 2. Shown in Fig. 2(a) are the lines along which the magnetic field is oriented within the conductor when the current is steady and constant. A dot represents a magnetic field coming toward the reader and a cross represents a magnetic field moving away from the reader. Figure 2(b) shows the induced current that is oriented to expel the changing flux in the conductor. The complete picture is presented in Fig. 2(c), where the two currents, i.e., the impressed and the induced currents, combine to give a current distribution that is quite nonuniform (9). The field and current distribution are limited to a small depth on the surface.

The nonuniform current distribution results in an increased resistance, which is especially significant at high frequencies. For the infinitely long cylinder of Fig. 2, this can be determined by solving the diffusion equation [Eq. (12)] in cylindrical coordinates. Only one component of the magnetic field exists for this problem, i.e., the azimuthal, and it is a function of only the radius. Only the axial component of the current density exists, and it too is a function of the radius. With these assumptions, the partial differential equation to be solved is given by

$$\frac{\partial}{\partial r}\left[\frac{1}{r}\frac{\partial}{\partial r}(rH_\phi)\right] = \mu_0\sigma\frac{\partial H_\phi}{\partial t} \tag{23}$$

Since the time-harmonic solution is sought, it is assumed that the magnetic field intensity can be represented by the form of Eq. (17). With that assumption the partial differential equation (23) can be converted to differential equation (24):

$$r^2\frac{d^2\tilde{H}_\phi}{dr^2} + r\frac{d\tilde{H}_\phi}{dr} - (1 - j\omega\mu_0\sigma r^2)\tilde{H}_\phi = 0 \tag{24}$$

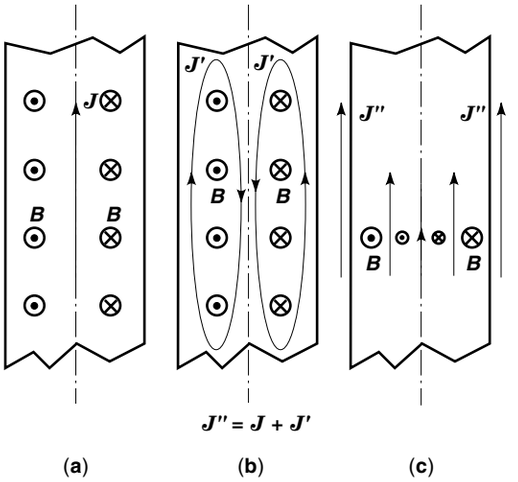

Figure 2. Physical explanation of the skin effect in a cylindrical conductor. (a) An impressed steady current density $\boldsymbol{J}$ and its magnetic field; (b) if the current/magnetic field were to increase, the induced currents J' would increase; (c) the induced current would subtract from the impressed current in the central region of the conductor and add to it on the outer periphery.

The solution to this equation, which remains finite at $r = 0$, is given by

$$\tilde{H}_\phi(r) = \tilde{C}_1 I_1(\alpha r) \tag{25}$$

Here α has the same definition as given in Eq. (19) and I_1 is the modified Bessel function (10,11) of the first kind of order one. Applying the boundary condition at $r = r_0$, i.e., $\tilde{H}_\phi(r_0) = I/2\pi r_0$ (here r_0 is the radius of the cylindrical conductor and I is the peak value of the total current flowing through the conductor), the solution is obtained as

$$\tilde{H}_\phi(r) = \frac{I I_1(\alpha r)}{2\pi r_0 I_1(\alpha r_0)} \tag{26}$$

and the current density is given by

$$\tilde{J}_z(r) = \frac{\alpha I I_0(\alpha r)}{2\pi r_0 I_1(\alpha r_0)} \tag{27}$$

The loss in the conductor per unit axial length is given by Eq. (12):

$$Q = \frac{1}{2}\int_0^{2\pi}\int_0^{r_0} \frac{\tilde{J}_z \tilde{J}_z^*}{\sigma}\, r\, dr\, d\phi \tag{28}$$

Here the * on J_z indicates the complex conjugate of the quantity. Evaluating this integral using identities related to the Bessel functions and recognizing the dc resistance of the cylindrical conductor as $R_{dc} = 1/\pi r_0^2 \sigma$, the ratio of ac to dc resistance of the conductor is given by

$$\text{Ratio} = \frac{R_{\text{ac}}}{R_{\text{dc}}} = \frac{1}{2}\frac{r_0}{\delta}\text{Re}\left[(1+j)\frac{I_0\left(\frac{r_0}{\delta}(1+j)\right)}{I_1\left(\frac{r_0}{\delta}(1+j)\right)}\right] \tag{29}$$

This function (29) is plotted in Fig. 3, with the quantity r_0/δ as a parameter. This curve shows that if the skin depth is small relative to the radius r_0, then the ratio is large.

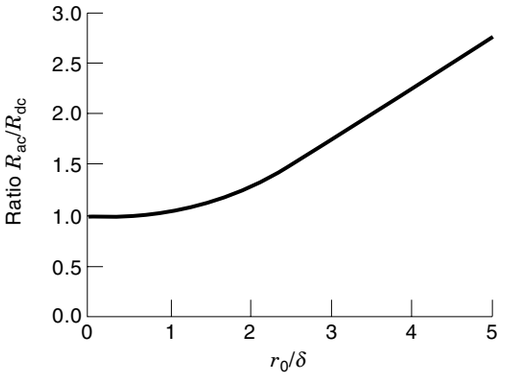

Figure 3. The ac to dc resistance ratio varies with frequency, becoming quite high at very high frequencies.

PROXIMITY EFFECT

The higher resistance and losses of the previous section were related with eddy currents induced in a conductor by the magnetic fields produced by the currents flowing in that conductor itself. Similarly, a conductor may experience a changing magnetic field due to currents changing in another conductor or set of conductors. The flow of eddy currents due to the externally produced changing magnetic fields is called the proximity effect. The classic example of this situation is when one phase of a three-phase power cable experiences the skin effect due to the alternating current that it carries and the proximity effect due to the alternating current carried by its two neighbors. For illustrative purposes the example chosen is that of a set of conductors placed in a slot of the stator of a rotating electrical machine, as shown in Fig. 4.

Shown alongside in Fig. 4 is the leakage (flux jumping across the slot) flux density as a function of slot depth. The Nth conductor experiences the magnetic field produced by the $N-1$ conductors below it in the slot (shown at the bottom of Fig. 4). For the purpose of simplification (to make the problem one-dimensional), it is further assumed that the conductor is much longer along the direction of the magnetic field. The coordinate system along with the conductor and the magnetic field is shown in Fig. 5.

Once again Eqs. (16) through (19) apply. The boundary conditions are different, however, and are given by $\tilde{H}_y(x) = H_0$ at $x = \pm d/2$. The solution is found by simple algebraic manipulation as

$$\tilde{H}_y(x) = H_0 \frac{\cosh(\alpha x)}{\cosh(\alpha d/2)} \tag{30}$$

$$\tilde{J}_z(x) = \alpha H_0 \frac{\sinh(\alpha x)}{\cosh(\alpha d/2)} \tag{31}$$

Here α has the same definition as in Eq. (19). Note that if Eq. (31) for the current density is integrated over the surface, the net current flow is zero, as it should be, since it has been assumed at the outset that the conductor has no net current in it. The power loss in the conductor per unit height and per unit depth can be calculated using the relation

$$Q = \frac{1}{2}\int_{-\frac{d}{2}}^{\frac{d}{2}} \frac{\tilde{J}_z \tilde{J}_z^*}{\sigma}\, dx \tag{32}$$

Substituting from Eq. (31) into Eq. (32) and performing the integral, the loss is obtained as

$$Q = \frac{H_0^2}{\sigma\delta}\left[\frac{\sinh\left(\frac{d}{\delta}\right) - \sin\left(\frac{d}{\delta}\right)}{\cosh\left(\frac{d}{\delta}\right) + \cos\left(\frac{d}{\delta}\right)}\right] \tag{33}$$

Equation (33) can now be used to introduce two important concepts, those of *inductively limited eddy currents* and *resistively limited eddy currents* (13). Whenever the magnetic field produced by the eddy currents is negligible in comparison to the applied magnetic field, then the eddy currents are termed *resistively limited.* The magnetic field can be low either because the current itself is small or because there is some other impediment to establishing the magnetic field. Resistively limited eddy currents are usually related to low frequencies where the eddy currents are small and do not significantly alter the applied magnetic field passing through the

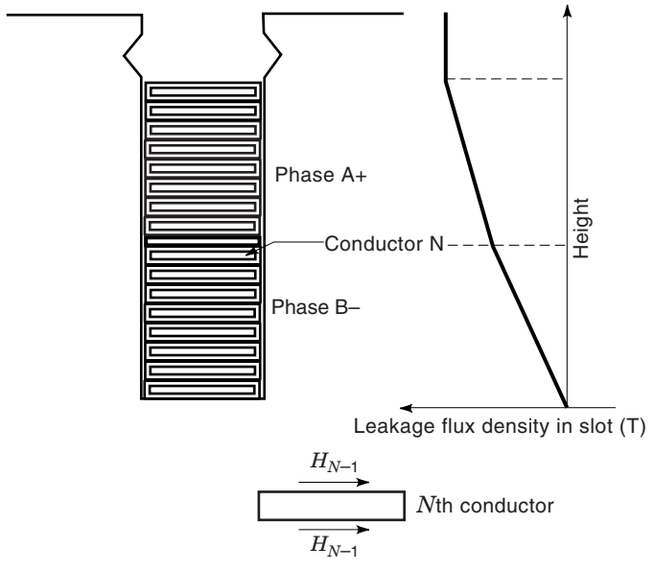

Figure 4. Proximity effect in the conductors placed in the slots of rotating electrical machinery.

conductor. When the magnetic field produced by the eddy currents is significant and must be considered in determining the total magnetic field, the eddy currents are termed *inductively limited.* Inductively limited eddy currents are usually related to high frequencies where the applied magnetic field is excluded from the conductor by large eddy currents flowing on the skin of the conductor.

Consider now two extreme cases which result in some simplification of Eq. (33). First consider the high-frequency limit when the skin depth δ is very small, thus resulting in a very high ratio d/δ. The hyperbolic terms in the square bracket of Eq. (33) dominate, since the trigonometric terms are limited to be ≤ 1. For large values of the arguments, the sinh and cosh terms are almost equal, thus giving the high-frequency limit to the loss as

$$Q = \frac{H_0^2}{\sigma\delta} \quad \text{for} \quad d \gg \delta \tag{34}$$

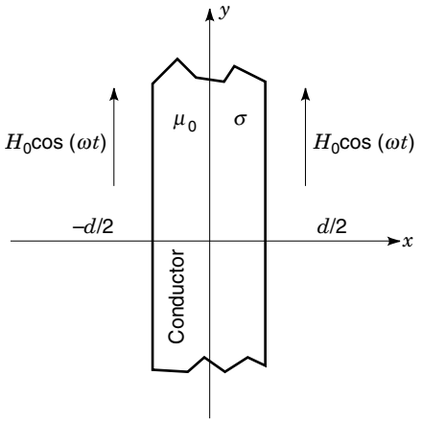

Figure 5. A conductor of finite thickness d immersed in an externally applied time harmonic field.

At very low frequencies the skin depth is large and the ratio d/δ is small. For this case the hyperbolic and trigonometric terms of Eq. (33) can be expanded in a Taylor series and all but the first two terms of the series can be dropped. When this approximation is made the loss is given by

$$Q = \frac{H_0^2}{\sigma\delta}\frac{1}{6}\left(\frac{d}{\delta}\right)^3 \tag{35}$$

or, rewriting Eq. (35) with the skin depth term expanded, $Q = \sigma B_0^2 \omega^2 d^3/24$, where $B_0 = \mu_0 H_0$.

The limit of the validity of the different equations can be understood by considering Fig. 6. In Fig. 6 the loss obtained from Eqs. (33) through (35) is plotted with respect to the ratio d/δ after normalizing with respect to the losses for the inductively limited case. For $d/\delta > 4$ the inductively limited formula gives good agreement with the exact solution. For $d/\delta < 1.6$ the resistively limited formula agrees well with the exact solution. In between these extremes one has to use the exact formula.

It must be noted that for the inductively limited case the losses are inversely proportional to the skin depth. This means that the losses increase proportionally to the square root of the frequency. An important fact can be derived from the resistively limited case of Eq. (35), namely, the losses are extremely sensitive to the thickness of the conductor in this regime. Ferromagnetic cores used in electrical machinery where an alternating magnetic field is present are laminated very finely for this reason. At high power frequencies (400–1000 Hz) the thickness may be as low as 0.15 mm. Making the laminations thinner also affects the magnetic properties adversely due to a loss of volume fraction. In the resistively limited regime it is preferable to have a low conductivity; therefore typical laminations will have silicon in the alloy to increase the resistivity of the material. For very high-frequency applications, cores are not made from iron or its alloys, but from ferrites that have inherently very low conductivity.

MOTION-RELATED EDDY CURRENTS

To understand motion-related eddy currents, an example of a rotating cylinder in a transverse magnetic field is considered.

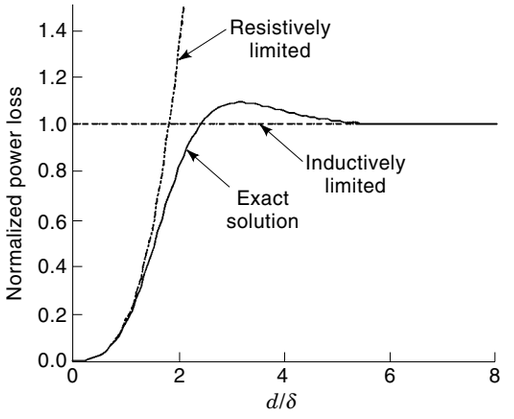

Figure 6. Losses in a conductor of thickness d in a time harmonic field: comparison of exact solution with low-frequency and high-frequency approximations.

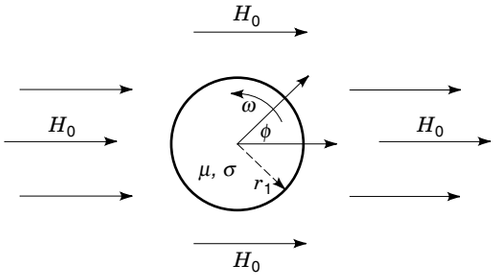

Figure 7. A rotating conducting cylinder in a transverse transient applied magnetic field.

The arrangement is shown in Fig. 7. To illustrate the analytical techniques a transient problem is selected. In this problem it is assumed that initially there is no magnetic field around or in the rotating cylinder, and at time $t = 0$ a magnetic field is instantaneously established around the rotating cylinder and diffuses into the cylinder. This applied field is in the form of a step, and the response obtained can be convolved for any other time variation of the applied magnetic field. The shaft of an air core rotating electrical machine with a stationary excitation coil, and the armature conductors of an air core machine, are some of the practical examples where this situation occurs.

It is assumed that the rotating cylinder is infinitely long, so that end effects are neglected. Thus the problem is two-dimensional. The conductor is assumed to have a conductivity of σ S/m, a permeability of μ Wb/(A/m), and a rotational speed of ω rad/s. The reference coordinate system is assumed to be stationary and the conductor to be moving relative to it. The cylindrical coordinate system is used for this problem because of symmetry. Equation (15) is valid within the conductor. Outside the conductor the equation to be solved is given by $\nabla^2 \boldsymbol{H} = 0$. The solutions in these two regions can be sought independently. However, they must obey the appropriate boundary conditions at the interface between the two regions. The boundary conditions are given as follows:

$$\begin{aligned} &\text{At } r = r_1: \quad H_{r1} = H_{r2} \\ &\qquad\qquad\quad H_{\phi 1} = H_{\phi 2} \\ &\text{At } r = 0: \quad H_{r1} \quad \text{and} \quad H_{\phi 1} \quad \text{are finite} \\ &\text{At } r \to \infty: \quad H_{r2} \quad \text{and} \quad H_{\phi 2} \quad \text{are finite} \end{aligned} \tag{36}$$

The first boundary condition, at the conductor–air interface, results from the continuity of the normal component of the magnetic field strength at the boundary. The second one results from the continuity of the magnetic field intensity, since it is assumed that there are no current sheets at the boundary. The other boundary conditions result from maintaining the physical quantities finite.

Consider the conductive region (region 1) first. The left-hand side of Eq. (15) ($\nabla^2 \boldsymbol{H} = -\nabla \times \nabla \times \boldsymbol{H}$) in cylindrical coordinates is given by

$$\begin{aligned} -\nabla \times \nabla \times \boldsymbol{H} = &-\frac{1}{r^2}\left[\frac{\partial}{\partial r}\left\{r\frac{\partial H_\phi}{\partial \phi}\right\} - \frac{\partial^2 H_r}{\partial \phi^2}\right]\boldsymbol{a}_r \\ &+ \frac{\partial}{\partial r}\left[\frac{1}{r}\left\{\frac{\partial}{\partial r}(rH_\phi) - \frac{\partial H_r}{\partial \phi}\right\}\right]\boldsymbol{a}_\phi \end{aligned} \tag{37}$$

Here $\boldsymbol{a}_r$ and $\boldsymbol{a}_\phi$ are the unit vectors along the radial and tangential directions.

The first term on the right-hand side in its components is given by

$$\frac{\partial \boldsymbol{H}}{\partial t} = \frac{\partial H_r}{\partial t}\boldsymbol{a}_r + \frac{\partial H_\phi}{\partial t}\boldsymbol{a}_\phi \tag{38}$$

Consider now the second term on the right-hand side. It is apparent that the velocity only has a tangential component $\boldsymbol{v} = r\omega\boldsymbol{a}_\phi$. The second term is

$$(\boldsymbol{v} \cdot \nabla)\boldsymbol{H} = \omega\frac{\partial H_r}{\partial \phi}\boldsymbol{a}_r + \omega\frac{\partial H_\phi}{\partial \phi}\boldsymbol{a}_\phi \tag{39}$$

Combining Eqs. (37) to (39), the two component equations are

$$-\frac{1}{r^2}\left[\frac{\partial}{\partial r}\left\{r\frac{\partial H_\phi}{\partial \phi}\right\} - \frac{\partial^2 H_r}{\partial \phi^2}\right] = \mu_0\sigma\left[\frac{\partial H_r}{\partial t} + \omega\frac{\partial H_r}{\partial \phi}\right] \quad \text{radial} \tag{40}$$

$$\frac{\partial}{\partial r}\left[\frac{1}{r}\left\{\frac{\partial}{\partial r}(rH_\phi)\right\} - \frac{\partial H_r}{\partial \phi}\right] = \mu_0\sigma\left[\frac{\partial H_\phi}{\partial t} + \omega\frac{\partial H_\phi}{\partial \phi}\right] \quad \text{tangential} \tag{41}$$

To simplify the analysis, the Laplace transform of the partial differential equation is performed with respect to the variable t (time), with the assumption that initially all the field quantities are zero. Considering the symmetry of the problem, it is assumed that the variation of the magnetic field intensity along the tangential direction is periodic and can be represented as follows:

$$\begin{aligned} H_r(r, \phi, t) &= \text{Re}[\tilde{H}_r(r, t)e^{j\phi}] \\ H_\phi(r, \phi, t) &= \text{Re}[\tilde{H}_\phi(r, t)e^{j\phi}] \end{aligned} \tag{42}$$

Use is made of the solenoidal property of the magnetic field strength ($\nabla \cdot \boldsymbol{B} = 0$). Since the material of the conductor is assumed to be *homogeneous*, $\nabla \cdot \boldsymbol{H} = 0$, which in cylindrical quantities gives

$$\frac{\partial H_\phi}{\partial \phi} = -\frac{\partial}{\partial r}(rH_r) \tag{43}$$

Substituting Eqs. (42) and (43) into Eq. (40) and transforming the time dependence to the frequency domain, the following equation is obtained:

$$r^2\frac{\partial^2 \tilde{H}_r}{\partial r^2} + 3r\frac{\partial \tilde{H}_r}{\partial r} = r^2(\mu_0\sigma s + j\omega\mu_0\sigma)\tilde{H}_r \tag{44}$$

Here as before the tilde denotes a complex quantity. This equation is in reality a total differential equation with a solution of the form

$$\tilde{H}_r(r, \phi, s) = \frac{1}{r}[\tilde{C}_1 J_1(pr) + \tilde{C}_2 Y_1(pr)]e^{j\phi} \tag{45}$$

where $p^2 = -\mu_0\sigma s - j\omega\mu_0\sigma$. Here J_1 and Y_1 are Bessel's function (10,11) of the first and second kind of order one. Using

Eqs. (37), (42), and (43) the solution in the nonconductive region is given by

$$\tilde{H}_r(r,\phi,s) = \left[\tilde{D}_1 + \frac{\tilde{D}_2}{r^2}\right] e^{j\phi} \tag{46}$$

The boundary conditions can now be used to determine the various constants. To keep the field finite within the conducting region $\tilde{C}_2 = 0$. It must be noted that $\lim_{z\to 0} J_1(z/z) = 1/2$, which means that the field remains finite at $r = 0$.

As r approaches infinity in the nonconducting region the effect of the perturbation caused by the rotating cylinder diminishes and the field is uniform, so that the far field is $H_r(r, \phi) = H_0 \cos(\phi)$. This indicates that constant $\tilde{D}_1 = H_0/s$. The remaining two constants are determined by applying the two boundary conditions of Eq. (36) at $r = r_1$. The boundary conditions at $r = r_1$ require the tangential component of the magnetic field, which can be obtained from Eq. (43) once the form of the radial component is determined.

The solution is as follows:

Region 1—conductor:

$$\tilde{H}_{r1}(r,\phi,s) = \frac{2H_0}{s}\frac{\left(\frac{r_1}{r}\right)J_1(pr)}{(pr_1)J_0(pr_1)}e^{j\phi} \tag{47}$$

$$\tilde{H}_{\phi 1}(r,\phi,s) = j\frac{2H_0}{s}\frac{\left(\frac{r_1}{r}\right)[(pr)J_0(pr) - J_1(pr)]}{(pr_1)J_0(pr_1)}e^{j\phi} \tag{48}$$

$$\tilde{J}_z(r,\phi,s) = -j\frac{2H_0}{s}\frac{pJ_1(pr)}{J_0(pr_1)}e^{j\phi} \tag{49}$$

Region 2—nonconductor:

$$\tilde{H}_{r2}(r,\phi,s) = \frac{H_0}{s}\left[\frac{(pr_1)J_0(pr_1) + \left(\frac{r_1}{r}\right)^2\{2J_1(pr_1) - (pr_1)J_0(pr_1)\}}{(pr_1)J_0(pr_1)}\right]e^{j\phi} \tag{50}$$

$$\tilde{H}_{\phi 2}(r,\phi,s) = j\frac{H_0}{s}\left[\frac{(pr_1)J_0(pr_1) - \left(\frac{r_1}{r}\right)^2\{2J_1(pr_1) - (pr_1)J_0(pr_1)\}}{(pr_1)J_0(pr_1)}\right]e^{j\phi} \tag{51}$$

The Inversion Integral

The expressions for the field quantities can be converted to the time domain using the inversion integral (14):

$$f(t) = \frac{1}{2\pi j}\int_{\alpha-j\infty}^{\alpha+j\infty} e^{st}F(s)\,ds \tag{52}$$

Here the path of integration is the Bromwich path and is such that α is greater than the largest real part of the poles of the integrand. To evaluate the integral, it is necessary to determine the poles of the transforms of the field quantities.

All the field quantities have poles corresponding to $s = 0$. Evaluation of the residues at this pole yields an expression that corresponds to the steady-state response to a step excitation. The other set of poles corresponds to the zeros of $J_0(pr_1)$. Bessel's function J_0 has an infinite number of real zeros z_n. The poles of $F(s)$ are thus obtained from $pr_1 = z_n$. The poles are thus given by

$$s_n = -\frac{\left(\frac{z_n}{r_1}\right)^2}{\mu_0\sigma} = -j\omega$$

Once the poles of the integrand have been determined, the solution in the time domain can be obtained as an infinite sum: $f(t) = \text{res}_{s=0}(F(s)) + \sum_{n=1}^{\infty} e^{s_n t}\,\text{res}_{s=s_n}(F(s))$ (15). Here res implies the residue of the argument at the corresponding pole. This inversion integral may be applied to each of the electromagnetic quantities to obtain an expression in the time domain. This procedure is fairly straightforward and amenable to evaluation.

Figure 8 shows the diffusion process in a rotating cylinder at various times until steady state is achieved. The magnetic Reynolds number (6) for this example is

$$R_m = \frac{\mu_0\sigma\omega r_1^2}{2} \approx 5 \tag{53}$$

Figure 9 shows the same process in a stationary cylinder. The magnetic field is directed tangential to the contours of constant magnetic vector potential shown in Figs. 8 and 9. It is seen that initially there is very little difference in the magnetic field orientation between the stationary and rotating cylinders. However, as steady state approaches, the magnetic field shows a swirling pattern with the rotating cylinder. In

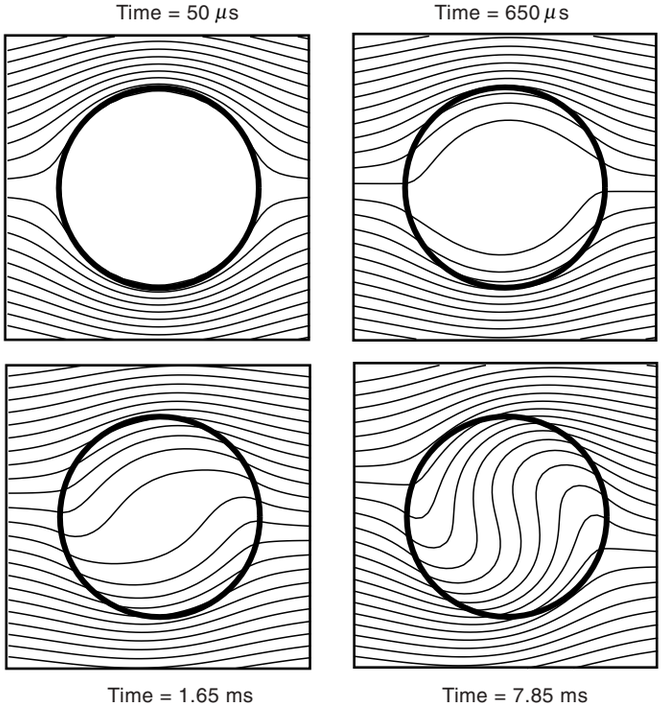

Figure 8. Transient magnetic diffusion in a solid conductive cylinder spinning in a transverse magnetic field.

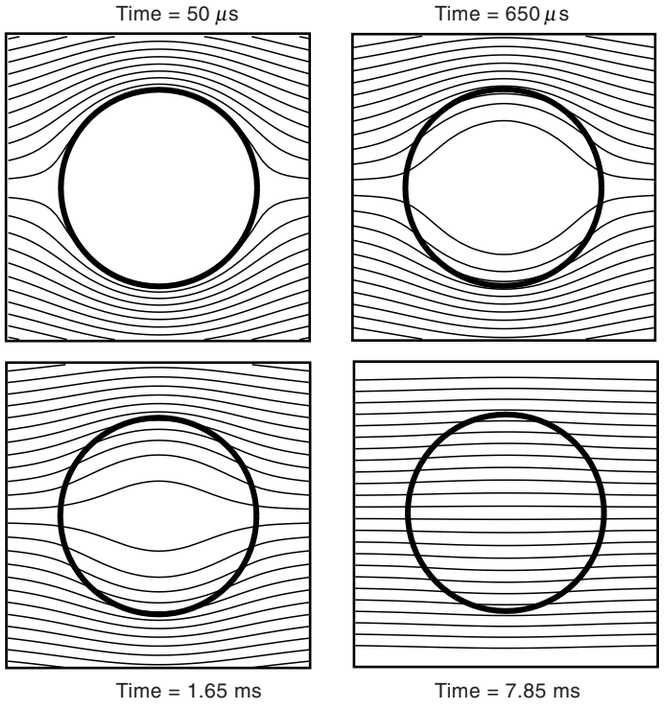

Figure 9. Transient magnetic diffusion in a solid conductive cylinder in a transverse magnetic field.

an attempt to minimize the rate of change of field, the rotating conductor attempts to drag the field in the direction of motion. This swirling of the magnetic field in the direction of motion results in a braking torque on the rotating cylinder. Figure 10 shows a typical torque versus speed curve under steady-state conditions, i.e., after the field is established and the rotor is spinning at a constant speed.

The braking action is used in devices such as induction motors and generators. In these devices, a rotating magnetic field is established by a multiphase stator winding. When the rotor (rotating cylinder) spins slower than the stator field, a torque acts on it to speed it up, thus providing motoring action. If the rotor spins faster than the stator field, then a torque acts on it to slow it down, providing generating action. Figure 10 also shows two other curves. These two curves are approximations to the exact solution when the magnetic

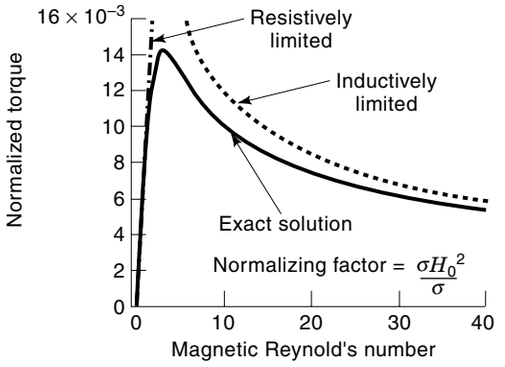

Figure 10. Typical torque curve for induction machines.

Reynolds number is very small (resistively limited eddy currents) or when it is very large (inductively limited eddy currents). The expression for power loss under these conditions is obtained as follows.

Resistively Limited Eddy Current

With this case the applied magnetic field is unaltered by the eddy currents. The electric field strength in the conductor is given by $\boldsymbol{E} = \boldsymbol{v} \times \boldsymbol{B}$. Since the velocity is tangential, only the axial component of the electric field exists:

$$E_Z = r\omega B_0 \cos(\phi)$$

The current density in the conductor is given by

$$J_Z = \sigma r\omega B_0 \cos(\phi) \tag{54}$$

The losses can thus be obtained by

$$Q = \int_0^{2\pi} \int_0^{r_1} \frac{J_z^2}{\sigma} r\, dr\, d\phi \ \text{W/m} \tag{55}$$

Carrying out the integration of Eq. (54) gives the following expression for losses in the rotating cylinder for the resistively limited case:

$$Q = \frac{\pi}{\sigma} H_0^2 R_{\mathrm{m}}^2 \ \text{W/m} \tag{56}$$

Here R_{m} is the magnetic Reynolds number as defined in Eq. (53). The torque can then be obtained by dividing the losses by the rotational speed, $\tau = Q/\omega$.

Inductively Limited Eddy Current

In this instance the eddy current flow is governed by the total field. The magnetic Reynolds number is quite large. The current tends to flow in a small skin depth on the surface of the conductor excluding the field from within the conductor. To exclude the field from the interior, the eddy currents must produce a magnetic field that is equal and opposite to the applied field within the conductor. A line current density on the surface given by $K_z = K_{mz} \sin(\phi)$, where $K_{mz} = 2H_0$, will produce an equal and opposite magnetic field in the interior (16). Assuming the current flows in a thin layer, one skin depth on the surface: $J_z = (2H_0/\delta) \sin(\phi)$. Integrating the losses over the cross section of the conductor, as in Eq. (55), the loss is obtained as

$$Q = \frac{4\pi}{\sigma} H_0^2 \sqrt{R_{\mathrm{m}}} \ \text{W/m} \tag{57}$$

Initially when the magnetic Reynolds number is small, the losses increase the square of the magnetic Reynolds number, and for high values as the square root. The above examples serve to illustrate the behavior of the eddy currents in the different regimens.

ANISOTROPIC CONDUCTORS

Pulsed electrical machines such as the compensated pulsed alternator (17) (compulsator) are increasingly being consid-

ered for mobile applications. Size and weight reduction in these machines is therefore very important. Composite materials, such as carbon fiber and glass fiber epoxy composites, with high strength and low density are a natural choice for the various structural components of these electrical machines. The carbon fiber–epoxy composite (CFC) is particularly useful because of its high strength and modulus. However, CFC is electrically conductive with vastly different electrical conductivities along the fibers and transverse to the fibers (18,19). When these materials are used in pulsed machines, it is important that the designer be cognizant of the conductivity and treat the anisotropy adequately. This section illustrates how the eddy current distribution can be determined in carbon filter composites in light of the anisotropy.

Use of the composite material has significantly enhanced the energy density. However, since iron cannot be used in the magnetic circuit to channel the flux, the excitation requirements increase significantly. This problem is usually overcome by pulse charging the field coil and minimizing the time that the field coil is on. Pulse charging necessitates that the eddy currents be properly accounted for.

Eddy currents will be generated by two mechanisms. The first one is motion related, due to the relative motion between the excitation field and the rotor (in the rotating armature configuration) or the stator (in the rotating field configuration). The second mechanism is due to rapidly changing magnetic field during a typical high-current discharge. The focus here is on the motion-related eddy currents, since typically this represents the larger loss. The purpose of this section is primarily to indicate a means of treating eddy currents in anisotropic materials.

Three types of fiber composites are usually considered. The glass–epoxy composites are the least expensive and are used for relatively low-strength applications. For high-strength applications carbon epoxy composites are preferred not only because they are stronger but also carbon fibers are inexpensive relative to the boron fibers. In some applications significant transverse strengths may be required, and in those instances boron fibers are used, especially if the transverse strength or stiffness cannot be imparted by longitudinal plies.

When these fibers are applied to the rotors of electrical pulsed machines, the greatest strength is needed in the hoop (azimuthal) direction since the majority of the centrifugal as well as discharge loading causes high hoop stress. The fibers are therefore predominantly oriented in the hoop direction. There may be a few plies of small radial thickness oriented axially to provide some axial stiffness and impart transverse strength.

Carbon fibers have an intrinsic electrical conductivity, and therefore one might expect that the composite material made from these fibers would be electrically conductive in the direction of the fibers. However, considerable transverse electrical conductivity is also observed. This transverse conductivity is a result of significant fiber-to-fiber contact. As might be expected, the longitudinal conductivity increases linearly with the fiber volume fraction. The transverse conductivity increases with the fiber volume fraction in a more complicated scaling relationship. Nominally below 30% to 40% fiber volume fraction, the transverse conductivity of graphite epoxy composites is almost zero (20). Table 2 summarizes typical conductivities for two fiber composites at a fiber volume fraction of about 60% to 70%.

Table 2. Typical Electrical Conductivities for Unidirectional Composites

Material	Longitudinal Conductivity (S/m)	Transverse Conductivity (S/m)
Graphite epoxy	20,000	200
Boron epoxy	30	2×10^{-8}

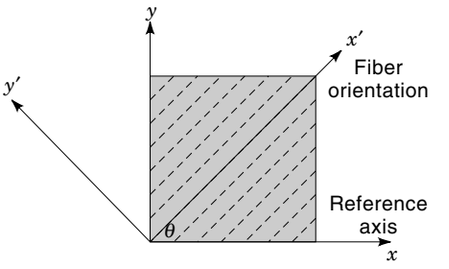

Figure 11. Relation between the principal axes, reference axes, and fiber orientation.

DISCUSSION OF ANISOTROPIC CONDUCTIVITY

The anisotropy ratio for the electrical conductivity is large along, and transverse to, the fibers. The electrical conductivity normal to the plane is also different, typically being half the transverse value. This difference comes about because most structures are fabricated by assembling several layers of the composite material. The contact between the fibers with adjacent subassemblies is not as good as within the assembly. This results in the electrical conductivity through the plane being somewhat lower. We therefore have to consider three different conductivities σ_1, σ_t, and σ_{cp} (i.e., longitudinal or along the fibers, transverse, and cross ply). For the present discussion and to simplify the analysis, we assume that the cross-ply conductivity is the same as the transverse conductivity and therefore restricts the eddy currents within a ply. Another assumption is that the eddy currents flowing in a plane thus have only x and y components. The relation between the current density and the electric field can now be written with the conductivity tensor:

$$[\boldsymbol{J}] = [\boldsymbol{\sigma}] \cdot [\boldsymbol{E}] \tag{58}$$

Assume for the moment that the fibers are aligned with the x axis. Equation (58) then can be expanded as follows:

$$\begin{bmatrix} J_x \\ J_y \end{bmatrix} = \begin{bmatrix} \sigma_1 & 0 \\ 0 & \sigma_t \end{bmatrix} \cdot \begin{bmatrix} E_x \\ E_y \end{bmatrix} \tag{59}$$

Here σ_1 is the conductivity along the fibers and σ_t is the conductivity transverse to the fibers. These reference axes, along which the conductivity matrix is diagonal, are called the principal axes. When the fibers are oriented at some arbitrary angle θ (as shown in Fig. 11) with respect to the x axis, the

conductivity matrix is no longer diagonal and there is cross coupling of the components. To derive this relation we make use of the rotation matrix, which relates the components in the primed coordinate system to the unprimed coordinate system.

$$[\boldsymbol{J}'] = [\boldsymbol{R}] \cdot [J], [\boldsymbol{E}'] = [\boldsymbol{R}] \cdot [E]$$
$$[\boldsymbol{R}] = \begin{bmatrix} \cos(\theta) & \sin(\theta) \\ -\sin(\theta) & \cos(\theta) \end{bmatrix} \tag{60}$$

In the primed coordinate system the conductivity matrix $[\sigma']$ is diagonal, as in Eq. (59). We can now derive the generalized conductivity matrix as follows:

$$[\boldsymbol{J}'] = [\boldsymbol{\sigma}'] \cdot [E']$$

Using Eq. (60), we get

$$[\boldsymbol{R}] \cdot [\boldsymbol{J}] = [\boldsymbol{\sigma}'] \cdot [\boldsymbol{R}] \cdot [E']$$

Further manipulation gives

$$[\boldsymbol{J}] = [\boldsymbol{R}]^{-1} \cdot [\boldsymbol{\sigma}'] \cdot [\boldsymbol{R}] \cdot [E']$$

and

$$[\boldsymbol{\sigma}] = [\boldsymbol{R}]^{-1} \cdot [\boldsymbol{\sigma}'] \cdot [\boldsymbol{R}]$$

(i.e., the generalized conductivity matrix).

Expanding and simplifying the equation gives

$$[\boldsymbol{\sigma}] = \begin{bmatrix} \sigma_l \cos^2(\theta) + \sigma_t \sin^2(\theta) & \dfrac{\sigma_l - \sigma_t}{2} \sin(2\theta) \\ \dfrac{\sigma_l - \sigma_t}{2} \sin(2\theta) & \sigma_l \sin^2(\theta) + \sigma_t \cos^2(\theta) \end{bmatrix} \tag{61}$$

Several features of the generalized conductivity matrix need to be noted:

1. The matrix is symmetric.
2. There are two angles, $\theta = 0°$ and $\theta = 90°$, for which the matrix is diagonal.
3. If $\sigma_1 = \sigma_{t\,(\text{isotropic})}$, then the off-diagonal terms vanish, as must be expected.

Figure 12 shows the variation of the elements in the matrix (61) as a function of the angle θ. This conductivity matrix

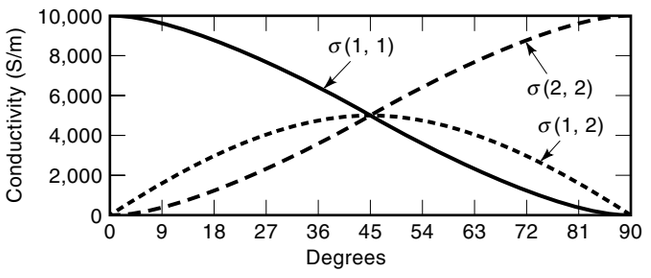

Figure 12. Variation of elements of conductivity matrix with angle of fibers.

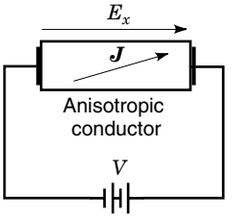

Figure 13. Mind experiment to understand conductivity matrix.

suggests that if we conduct the experiment shown in Fig. 13, where a potential difference V is applied across the vertical faces resulting in an electric field strength of E_x, there will not only be a current density along the x direction J_x but also a current density J_y due to the cross coupling in the conductivity matrix. The electric field vector and the current density vector are not collinear, as is to be expected in anisotropic materials.

MODEL FOR RESISTIVELY LIMITED EDDY CURRENTS IN ANISOTROPIC CONDUCTORS

Figure 14 shows the physical and analytical models for a ring spinning in a heteropolar magnetic field. To simplify the algebra, a planar model is assumed. This assumption is especially valid for thin rings at large radii. The magnetic field in the present case is established by the field coil, and it is assumed that this field remains steady. It is also assumed that the ring is spinning at a constant rotational speed ω with respect to the field; therefore, the steady-state eddy currents are being sought. The governing equations and boundary conditions are given in this section. For the present case it is assumed that the eddy currents are resistance limited. This implies that the magnetic field distribution is not significantly perturbed by the presence of the eddy currents. This assumption is valid at low frequencies with CFCs. This also allows one to make the assumption that the current distribution is not a function of the depth within the composite or, alternatively, that the skin depth at the operating frequency is much greater than the thickness of the sample. To keep this in perspective, consider a 25 mm CFC ring spinning in a dipole at 250 Hz. The skin depth in the CFC using the longitudinal conductivity is about 22.5 cm.

$$\nabla \times E = \nabla \times (v \times B) \quad \text{Maxwell's equation}$$
$$\nabla \cdot J = 0 \quad \text{Conservation of charge}$$
$$\begin{bmatrix} J_x \\ J_y \end{bmatrix} = \begin{bmatrix} \sigma_x & \sigma_{xy} \\ \sigma_{xy} & \sigma_y \end{bmatrix} \cdot \begin{bmatrix} E_x \\ E_Y \end{bmatrix} \quad \text{Constitutive relation}$$
$$J_y = 0 \quad \text{at} \quad y = \pm a \quad \text{Boundary conditions}$$

As shown in Fig. 14, the magnetic flux density varies sinusoidally along the x direction (azimuthally in the physical model). That is,

$$B_z = B_{zm} \sin\left(\frac{\pi}{L} x\right)$$

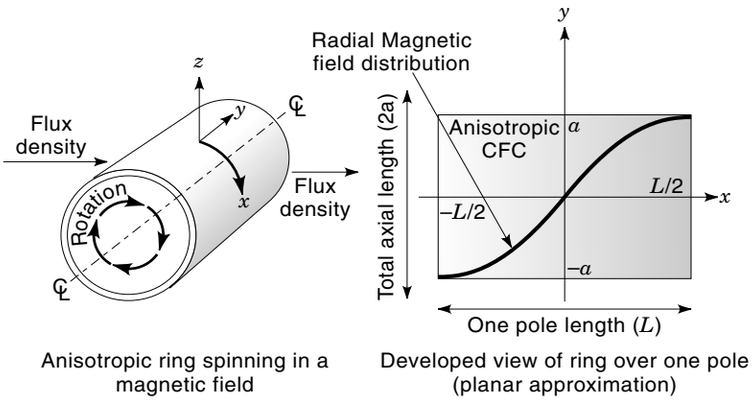

Figure 14. Physical and analytical models.

When we expand Maxwell's equation, we get the following partial differential equation:

$$\frac{\partial E_y}{\partial x} - \frac{\partial E_x}{\partial y} = \left(vB_{zm}\frac{\pi}{L}\right)\cos\left(\frac{\pi}{L}x\right) \tag{62}$$

In this equation v is the spin velocity of the sample in m/s.

After inverting the conductivity matrix, we get the resistivity matrix:

$$\begin{bmatrix} E_x \\ E_y \end{bmatrix} = \begin{bmatrix} \rho_x & \rho_{xy} \\ \rho_{xy} & \rho_y \end{bmatrix} \cdot \begin{bmatrix} J_x \\ J_y \end{bmatrix} \tag{63}$$

Substituting Eq. (63) in Eq. (62) on the right-hand side, we get

$$\frac{\partial E_y}{\partial x} - \frac{\partial E_x}{\partial y} = \rho_{xy}\frac{\partial J_x}{\partial x} + \rho_y\frac{\partial J_y}{\partial x} - \rho_x\frac{\partial J_x}{\partial y} - \rho_{xy}\frac{\partial J_y}{\partial y} \tag{64}$$

Substituting Eq. (64) in Eq. (62) and differentiating with respect to x, we get

$$\rho_{xy}\frac{\partial^2 J_x}{\partial x^2} + \rho_y\frac{\partial^2 J_y}{\partial x^2} - \rho_x\frac{\partial^2 J_x}{\partial x\,\partial y} - \rho_{xy}\frac{\partial^2 J_y}{\partial x\,\partial y} = -vB_{zm}\left(\frac{\pi}{L}\right)^2\sin\left(\frac{\pi}{L}x\right) \tag{65}$$

This expression assumes that the conductivity does not vary with the coordinates.

We now make use of the equation for the conservation of charge to get

$$\nabla \cdot J = 0 \Rightarrow \frac{\partial J_x}{\partial x} + \frac{\partial J_y}{\partial y} = 0$$

Now differentiate once w.r.t. x and then w.r.t. y to get

$$\begin{aligned} \frac{\partial^2 J_x}{\partial x^2} &= -\frac{\partial^2 J_y}{\partial y\,\partial x} \\ \frac{\partial^2 J_x}{\partial y\,\partial x} &= -\frac{\partial^2 J_y}{\partial y^2} \end{aligned} \tag{66}$$

Substituting Eq. (66) in Eq. (65), we get an expression in J_y only.

$$\left\{\rho_x\frac{\partial^2 J_y}{\partial y^2} + \rho_y\frac{\partial^2 J_y}{\partial x^2} - 2\rho_{xy}\frac{\partial^2 J_y}{\partial x\,\partial y}\right\} = -vB_{zm}\left(\frac{\pi}{L}\right)^2\sin\left(\frac{\pi}{L}x\right) \tag{67}$$

To solve this equation it is assumed that the solution takes the form

$$J_y = \mathrm{Im}[e^{j\alpha x}Y(y)] \tag{1}$$

$$\alpha = \frac{\pi}{L} \tag{2}$$

(i.e., that the solution is periodic along the x coordinate).

Applying the boundary conditions, we get the following solution:

$$J_y = \mathrm{Im}\left\{\frac{vB_{zm}}{\rho_y}e^{j\alpha x}\left[1 + e^{\gamma_1 y}\left(\frac{\sinh(\gamma_2 a)}{\sinh(2\eta a)}\right) - e^{\gamma_2 y}\left(\frac{\sinh(\gamma_1 a)}{\sinh(2\eta a)}\right)\right]\right\}$$

$$J_x = \mathrm{Im}\left\{j\frac{vB_{zm}}{\rho_y \alpha}e^{j\alpha x}\left[\gamma_1 e^{\gamma_1 y}\left(\frac{\sinh(\gamma_2 a)}{\sinh(2\eta a)}\right) - \gamma_2 e^{\gamma_2 y}\left(\frac{\sinh(\gamma_1 a)}{\sinh(2\eta a)}\right)\right]\right\}$$

$$\alpha = \pi/\text{pole pitch};\ 2a = \text{ axial length}$$

$$\gamma_1 = \eta + j\xi;\ \gamma_2 = -\eta + j\xi$$

$$\eta = \alpha\sqrt{\frac{\rho_x\rho_y - \rho_{xy}^2}{\rho x}}$$

$$\xi = \alpha\left(\frac{\rho_{xy}}{\rho_x}\right)$$

Figure 15 illustrates these equations for various fiber orientations. These plots assumed a transverse conductivity of 100 S/m and a longitudinal conductivity of 10,000 S/m. The contours represent the fraction of the total current per pole flowing within that contour. This implies that for contour lines closer together the current density is higher. Of particular interest is the distribution for the case when the fibers are all azimuthal (along the x axis) (i.e., when $\theta = 0$). This distribution shows a significant crowding of the contour lines and therefore a high current density near the axial ends of the cylinder. Figure 16 best explains the reason for this type of distribution. Consider the CFC cylinder as a set of cells along the axis. Each cell has a voltage applied due to the speed voltage and resistance along the axis but no resistance

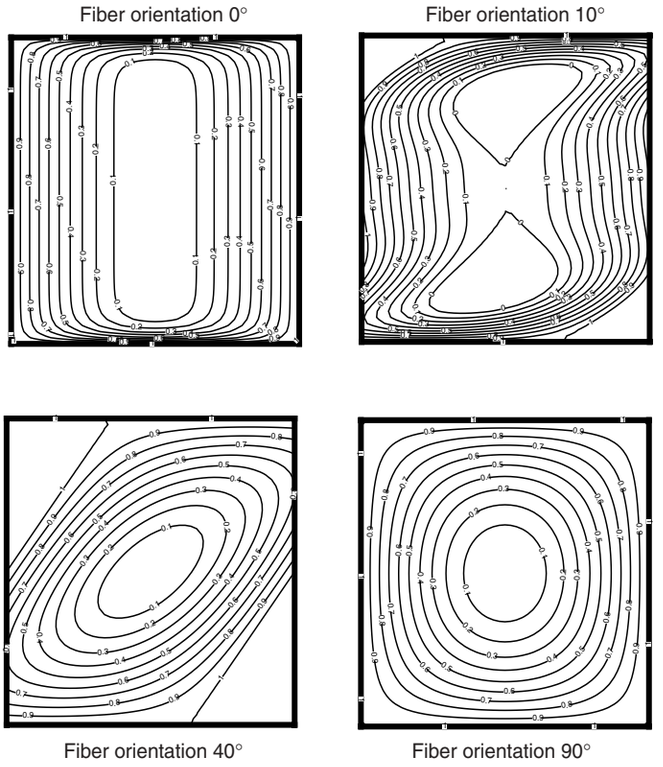

Figure 15. Eddy current distribution in a thin shell on the rotor surface—distribution for various fiber orientations.

along the azimuthal path. This is justified by the high anisotropy ratio. Each cell has an equal current, with the result that on the paths where the cells overlap the currents cancel and there exists only an overall path through the axial ends of the CFC sample.

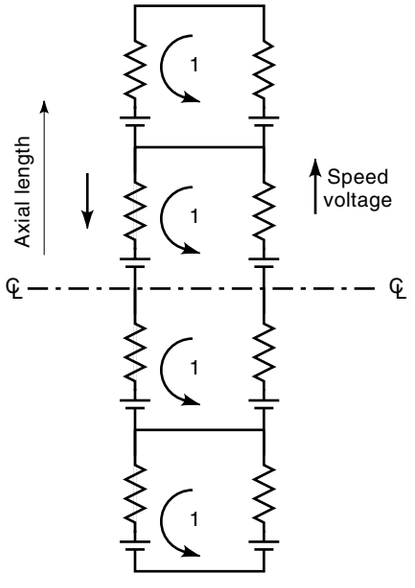

Figure 16. Interpretation of current distribution for the case $\theta = 0$.

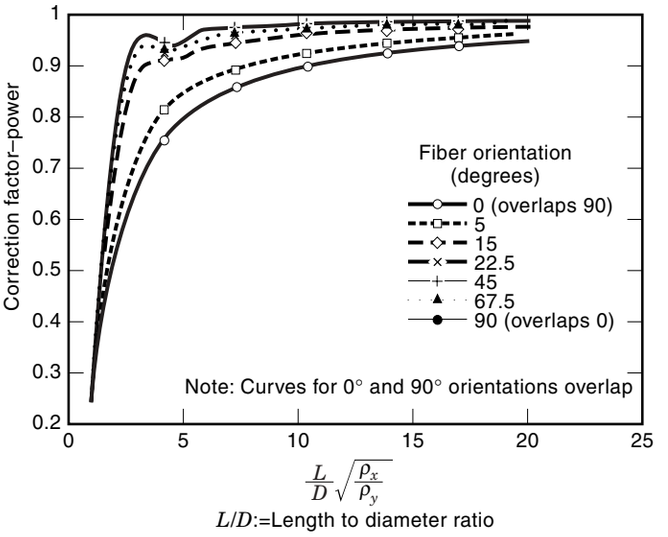

Figure 17. Correction factor to be applied for power loss calculations using the infinitely long cylinder formula (s_l = 10000 S/m and s_t = 100 S/m).

CALCULATION OF THE EDDY CURRENT LOSSES

As discussed earlier (Fig. 13), the $\boldsymbol{J}$ and $\boldsymbol{E}$ vectors are not collinear. One must therefore exercise caution in writing the expression for the losses. Using fundamental relations, the power loss can be expressed as

$$p = \boldsymbol{E} \bullet \boldsymbol{J} \quad (\mathrm{W/m^3}) \tag{68}$$

Therefore,

$$p = E_l J_l + E_t J_t$$

resolving components along and transverse to the fibers (principal axis) or, alternatively,

$$p = E_x J_x + E_y J_y$$

The two expressions are equivalent; however, we choose the expression based on the principal axis for the sake of convenience. The expression for the power loss is now

$$p = \frac{J_l^2}{\sigma_l} + \frac{J_t^2}{\sigma_t} \tag{69}$$

To obtain the total losses in the cylinder, one must perform the volume integral in Eq. (69). Considering the complexity in the expressions for current density, a numerical integration was performed with satisfactory results.

Figure 17 shows a plot of the total losses in an anisotropic cylinder for various fiber orientations and length to diameter ratio. The y axis has been normalized by the expression

$$P = \pi \sigma_y L (\omega B_{zm})^2 \frac{(r_o^4 - r_i^4)}{4} \tag{70}$$

Here ω is the rotational speed of the cylinder in radians per second, L is the total length of the cylinder, and r_o and r_i are

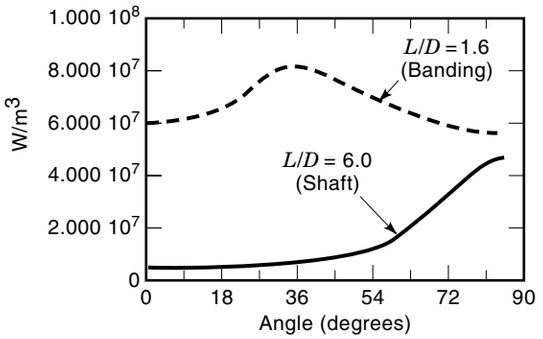

Figure 18. Variation of losses with fiber orientation and length to diameter ratio.

the outer and inner radii of the cylinder, respectively. Equation (70) is obtained when losses per meter are calculated for an infinitely long cylinder using the conductivity for current flow along the axis and then multiplying the loss per unit length by the axial length of the cylinder. It is then no surprise that all the losses approach Eq. (70) asymptotically as the L/D ratio continues to increase arbitrarily. However, it must be noted that the x axis is weighted by the square root of the conductivity ratio.

Figure 18 shows two curves one for a large L/D ratio and the other for a relatively small value. The low L/D application is for a component such as the outermost banding of a composite rotor. The large L/D is for the shaft of a similar machine. The loss has been plotted as a function of the fiber orientation, with 0° being purely azimuthal and 90° purely axial fibers. In several applications it may be necessary to provide some axial stiffness to the structure. This can be accomplished in two ways: (1) by having plies with purely axial fibers, and (2) by winding the fibers at an angle. Figure 18 indicates that to minimize the losses in the banding, the approach of axial plies might be better. The purpose of the shaft is to provide axial stiffness; however, that indicates that the fibers must be oriented at 90°, and therefore (according to Fig. 18) incur the highest losses of all the fiber orientations. To control the losses one might use a 60° ply.

GENERAL MODEL FOR EDDY CURRENTS IN ANISOTROPIC CONDUCTORS

The preceding discussion gives a good illustration of the manner in which eddy currents in anisotropic materials need to be treated. However, since the eddy currents considered are resistance limited, the application is restricted to resistive composites such as CFCs at relatively low frequencies. To extend the analytical capability to the general case of eddy currents in anisotropic material numerical techniques (21) such as finite element, boundary element, or finite difference methods must be used. These methods allow generalized constitutive relations, such as

$$\begin{bmatrix} J_x \\ J_y \\ J_z \end{bmatrix} = \begin{bmatrix} \sigma_{xx} & \sigma_{xy} & \sigma_{xz} \\ \sigma_{xy} & \sigma_{yy} & \sigma_{yz} \\ \sigma_{xz} & \sigma_{yz} & \sigma_{zz} \end{bmatrix} \cdot \begin{bmatrix} E_x \\ E_y \\ E_z \end{bmatrix} \tag{71}$$

When anisotropic materials with arbitrary material orientations are used, the matrix of Eq. (71) is full. Simple problems that with isotropic materials would be two-dimensional become three-dimensional because of the cross coupling of the electric field. A simple problem for illustrative purposes is that of a circular core probe inducing eddy currents on a material, as is typically used in nondestructive eddy current testing. It is found that in isotropic materials the path of the eddy currents is also circular; however, with unidirectional carbon fiber composites the circular probes result in an elliptical eddy current path with the major axis aligned with the fiber (higher conductivity). Typically the major axis is three times the minor axis (22). This effect is illustrated Fig. 19.

USE OF POTENTIALS IN CALCULATIONS OF EDDY CURRENTS

In the examples used above, most of the calculations have been performed using field quantities directly. Considerable reduction in computational effort is obtained, especially for three-dimensional problems, if the calculations are performed in terms of the potentials. There are two basic approaches that can be adopted when representing field quantities in terms of potentials. The first one uses the solenoidal property

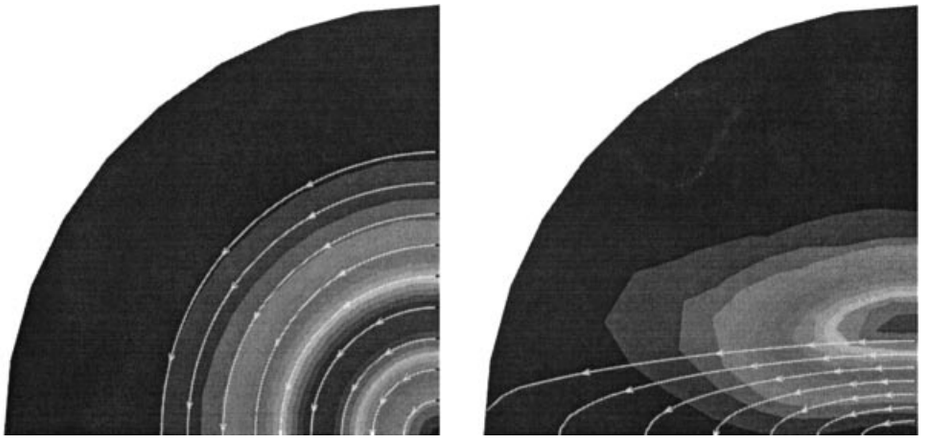

Figure 19. Comparison of patterns of induced current from a pulsed coil in (a) an isotropic conductor and (b) an anisotropic conductor with higher conductivity along the horizontal axis.

($\nabla \cdot \boldsymbol{B} = 0$) of the magnetic field strength vector and the second uses the solenoidal property ($\nabla \cdot \boldsymbol{J} = 0$) of the current density vector.

Starting with Eq. (7) and making use of the fact that the divergence of $\boldsymbol{B}$ is zero, we obtain

$$\boldsymbol{B} = \nabla \times \boldsymbol{A} \tag{72}$$

Here $\boldsymbol{A}$ is the magnetic vector potential. Substituting this into Faraday's law [Eq. (6)] gives

$$\nabla \times \left(\boldsymbol{E} + \frac{\partial \boldsymbol{A}}{\partial t} \right) = 0 \tag{73}$$

Using the identity that the curl of the gradient of a scalar field is zero, we obtain

$$\boldsymbol{E} = -\frac{\partial \boldsymbol{A}}{\partial t} - \nabla V \tag{74}$$

Here V is the electric scalar potential. Thus the electric field and the magnetic field are represented in terms of the potentials. Making use of the constitutive relationships [Eqs. (9) and (10)] and Ampere's law [Eq. (5)], the following equation is obtained in terms of potentials:

$$\nabla \times \frac{1}{\mu_0}(\nabla \times \boldsymbol{A}) = -\sigma \left(\frac{\partial \boldsymbol{A}}{\partial t} + \nabla V \right) \tag{75}$$

The two potentials $\boldsymbol{A}$ and V constitute four unknowns. Equation (75) in its components gives only three equations. One more equation is needed to solve for these unknowns. Equation (8) is the one chosen for most methods. This gives one additional equation relating $\boldsymbol{A}$ and V:

$$\nabla \cdot \left[\sigma \left(\frac{\partial \boldsymbol{A}}{\partial t} + \nabla V \right) \right] = 0 \tag{76}$$

It must be noted that $\boldsymbol{A}$ is not uniquely defined as yet, since only its curl is defined; however, to define uniquely a vector field, its curl as well as its divergence need to be known. Defining the divergence is termed selecting a *gauge condition* (23,24,25). Two gauge conditions commonly used are

$$\nabla \cdot \boldsymbol{A} = 0 \quad \text{Coulomb gauge} \tag{77}$$

$$\nabla \cdot \boldsymbol{A} = -\mu_0 \sigma V \quad \text{Lorentz gauge} \tag{78}$$

In a linear material with constant permeability, Eqs. (75) and (76) become

$$\nabla^2 \boldsymbol{A} = \mu_0 \sigma \left(\frac{\partial \boldsymbol{A}}{\partial t} + \nabla V \right) \qquad \text{with Coulomb gauge} \tag{79}$$
$$\nabla^2 V = 0$$

$$\nabla^2 \boldsymbol{A} = \mu_0 \sigma \frac{\partial \boldsymbol{A}}{\partial t} \qquad \text{with Lorentz gauge} \tag{80}$$
$$\nabla^2 V = \mu_0 \sigma \frac{\partial V}{\partial t}$$

It is worth noting that with the Coulomb gauge the two potentials are coupled; however, the equation for the electric scalar potential is a simple Laplacian. With the Lorentz gauge the two potentials are decoupled, and both follow the diffusion equation.

Using Eq. (8) as the starting point, a different set of potentials is obtained (26,27). Once again, since its divergence is identically zero, the current density may be represented as

$$\boldsymbol{J} = \nabla \times \boldsymbol{T} \tag{81}$$

Here $\boldsymbol{T}$ is the electric vector potential. Substituting Eq. (81) in Eq. (5) gives

$$\nabla \times (\boldsymbol{H} - \boldsymbol{T}) = 0 \tag{82}$$

Since a vector whose curl is identically zero is the gradient of a scalar,

$$\boldsymbol{H} = \boldsymbol{T} - \nabla \Omega \tag{83}$$

Here Ω is the magnetic scalar potential. Substituting Eq. (83) into Eq. (6) and using the constitutive relations Eqs. (9) and (10) gives

$$\nabla \times \frac{1}{\sigma} \nabla \times \boldsymbol{T} = -\mu_0 \left(\frac{\partial \boldsymbol{T}}{\partial t} - \nabla \frac{\partial \Omega}{\partial t} \right) \tag{84}$$

The second equation with this method is Eq. (7) implemented with the potentials

$$\nabla \cdot \mu_0 (\boldsymbol{T} - \nabla \Omega) = 0 \tag{85}$$

For the uniqueness of the electric vector potential, the Coulomb gauge is usually implemented, i.e., $\nabla \cdot \boldsymbol{T} = 0$.

The duality in the two approaches is quite apparent. There are some obvious advantages and disadvantages of these two approaches that become strongly evident when these equations are solved by numerical methods. The magnetic vector potential method satisfies Eq. (7) more accurately, but Eq. (8) is satisfied only approximately, and the opposite is true with the electric scalar potential implementation. Both these methods have been adopted in solving eddy current problems.

BIBLIOGRAPHY

1. R. S. Elliot, *Electromagnetics—History, Theory, and Applications,* Piscataway, NJ: IEEE Press 1993, chap. 5, pp. 256–264.
2. W. D. Stevenson, Jr., *Elements of Power System Analysis,* 3rd ed., Tokyo: McGraw-Hill Kogakusha Ltd., 1975, chap. 2, pp. 39–40.
3. J. F. Gieras, *Linear Induction Drives,* Oxford, UK: Clarendon, 1994, chap. 1, pp. 1–33.
4. P. Lorrain and D. R. Corson, *Electromagnetic Fields and Waves,* 2nd ed., San Francisco, CA: W. H. Freeman, 1970, chap. 10, pp. 422–458.
5. H. H. Woodson and J. R. Melcher, *Electromechanical Dynamics, Pt. 1: Discrete Systems,* New York: Wiley, 1968, appendix B, pp. B1–B38.
6. J. R. Melcher, *Continuum Electromechanics,* Cambridge, MA: MIT Press, 1981, chap. 6, pp. 6.1–6.39.
7. J. A. Tegopolous and E. E. Kreizis, *Eddy Currents in Linear Conducting Media,* Amsterdam: Elsevier, 1985, chap. 3, p. 19.
8. J. R. Reitz and F. J. Milford, *Foundations of Electromagnetic Theory,* 2nd ed., Reading, MA: Addison-Wesley, 1974, p. 80.
9. V. G. Welsby, *The Theory and Design of Inductance Coils,* New York: Wiley, 1960, chap. 3. pp. 46–54.
10. E. Kreyszig, *Advanced Engineering Mathematics,* New York: Wiley, 1979, chap. 11, p. 545.

11. M. Abramowitz and I. Stegun, *Handbook of Mathematical Functions,* New York: Dover, 1972, chaps. 9–11.
12. M. P. Perry, *Low Frequency Electromagnetic Design,* New York: Marcel Dekker, p. 140.
13. R. L. Stoll and P. Hammond, Calculation of the magnetic field of rotating machines. Pt. 4: Approximate determination of the field and the losses associated with eddy currents in conducting surfaces, *Proc. IEE,* **12**: 2083–2094, 1965.
14. R. V. Churchill, *Operational Mathematics,* New York: McGraw-Hill, 1972, pp. 193–218.
15. E. Kreyszig, *Advanced Engineering Mathematics,* New York: Wiley, 1979, pp. 723–737.
16. J. R. Bumby, *Superconducting Rotating Electrical Machinery,* Oxford, UK: Clarendon, 1983, p. 71.
17. M. L. Spann et al., Compulsator research at the University of Texas at Austin—an overview, *IEEE Trans. Magn.,* **25**: 529–537, 1989.
18. Rochester Institute of Technology, *A Technology Plan for Electromagnetic Characteristics of Advanced Composites,* Phase Report, July 1976, RADC-TR-76-206.
19. Georgia Institute of Technology, *Electromagnetic Properties and Effects of Advanced Composite Materials: Measurements and Modelling,* Phase Report, June 1978, RADC-TR-78-156.
20. J. Summerscales, Electrical and magnetic testing, in *Non-Destructive Testing of Fiber-Reinforced Plastics,* Amsterdam: Elsevier, vol. 2, chap. 5, p. 264.
21. E. E. Kriezis, et al., Eddy currents—Theory and applications. *Proc. IEEE,* **80**: 1559–1589, 1992.
22. R. Prakash, Eddy current testing, in *Non-Destructive Testing of Fiber Reinforced Plastics,* Amsterdam: Elsevier, vol. 2, chap. 6, pp. 299–325.
23. O. Biro and K. Preis, On the use of the magnetic vector potential in the finite element analysis of three-dimensional eddy currents, *IEEE Trans. Magn.,* **25**: 3145–3159, 1989.
24. C. F. Bryant, C. R. I. Emerson, and C. W. Trowbridge, A comparison of Lorentz gauge formulations in eddy current computations, *IEEE Trans. Magn.,* **26**: March, 1990.
25. K. J. Binns, P. J. Lawrenson, and C. W. Trowbridge, *The Analytical and Numerical Solution of Electric and Magnetic Fields,* New York: Wiley, 1992, chap. 12, pp. 366–379.
26. T. W. Preston and A. B. J. Reece, Solution of 3-dimensional eddy current problems: The T-Ω method, *IEEE Trans. Magn.,* **18**: 486–491, 1982.
27. J. Wang and B. Tong, Calculation of 3D eddy current problems using a modified T–Ω method, *IEEE Trans. Magn.,* **24**: 114–117, 1988.

Reading List

H. Knoepfel, *Pulsed High Magnetic Fields,* Amsterdam: North-Holland, 1970, chap. 3, Magnetic diffusion theory, chap. 4, Energy dissipation and nonlinear diffusion in pulsed magnetic fields.

A. Krawczyk and J. A. Tegopoulos, *Numerical Modelling of Eddy Currents,* Oxford, UK: Clarendon, 1993.

R. L. Stoll, *The Analysis of Eddy Currents,* Oxford, UK: Clarendon, 1974.

H. H. Woodson and J. R. Melcher, *Electromechanical Dynamics Pt. 2: Fields Forces and Motion,* Malabar, FL: Krieger, 1985, Section 7.1.1, Diffusion as an electrical transient.

S. B. PRATAP
The University of Texas at Austin